Discovery of a novel small molecule inhibitor of specific serine-residue BAD phosphorylation

Vijay Pandey[1,#], Wang Baocheng[1,2,#], Chakrabhavi Dhananjaya Mohan[3,#], Ainiah Rushdiana Raquib[4], Shobith Rangappa[5], Venkatachalaiah Srinivasa[6], Julian E. Fuchs[7], Kesturu S. Girish[8], Tao Zhu[9], Andreas Bender[7], Lan Ma[1], Zhinan Yin[2,11], Basappa[6,12,*], Kanchugarakoppal S. Rangappa[10,*], and Peter E. Lobie [1,4,*]

[1]*Tsinghua Berkeley Shenzhen Institute, Tsinghua University, Shenzhen 518055, China P.R.*
[2]*The first Affiliated Hospital, Biomedical Translational Research Institute, Jinan University, Guangzhou, China.P.R. 510632*
[3]*Department of Studies in Molecular Biology, University of Mysore, Manasagangotri, Mysore-570006, India*
[4]*Cancer Science Institute of Singapore, National University of Singapore, Singapore 117599*
[5]*Adichunchanagiri Institute for Molecular Medicine, Mandya District, India*
[6]*Laboratory of Chemical Biology, Department of Chemistry, Bangalore University, Bangalore 560001, India*
[7]*Centre for Molecular Informatics, Department of Chemistry, University of Cambridge, Cambridge, United Kingdom*
[8]*Department of Studies and Research in Biochemistry, Tumkur University, Tumkur 572103, India*
[9]*Hefei National Laboratory for Physical Sciences at Microscale and School of Life Sciences, University of Science and Technology of China, Anhui, P.R. China*
[10]*Institution of Excellence, University of Mysore, Manasagangotri, Mysore-570006, India*
[11]*National Center for International Research of Biological Targeting Diagnosis and Therapy, Guangxi Key Laboratory of Biological Targeting Diagnosis and Therapy Research, Collaborative Innovation Center for Targeting Tumor Diagnosis and Therapy, Guangxi Medical University, Nanning, 530021, P. R. China.*
[12]*Department of Studies in Organic Chemistry, University of Mysore, Manasagangotri, Mysore-570006, India*

[#]Contributed equally

*Corresponding authors

Correspondence to:
Basappa, email: salundibasappa@gmail.com
Kanchugarakoppal S. Rangappa, email: rangappaks@yahoo.com
Peter E. Lobie, email: pelobie@sz.tsinghua.edu.cn

Supporting information 1: A library of druggable small molecules

Scheme 1

The present scheme relates to a compound of Formula I

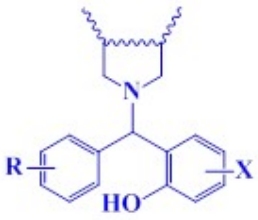

Formula I

Where: X=Cl; R=2-Cl; R=4-Cl; R=3-F & 4-C_6H_5-CH_2-O-; R= 3-CH_3-R= 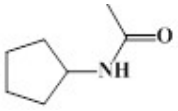

Where, 'R' is selected from the group comprising chlorine, methyl, fluorine and N-cyclopentylacetamido groups and X is selected from the group comprising chlorine and hydrogen; or its tautomers, isomers, analogues, derivatives or salts thereof.

the compound of Formula I is selected from group comprising:
(2-chlorophenyl)(4-(4-methoxyphenyl)piperazin-1-yl)methyl)phenol;
2-((4-chlorophenyl)(4-(4-methoxyphenyl)piperazin-1-yl)methyl)phenol;
2-((4-(benzyloxy)-3-fluorophenyl)(4-(4-methoxyphenyl)piperazin-1 yl)methyl)phenol;
(4-((2-hydroxyphenyl)(4-(4-Methoxyphenyl)piperazinyl)methyl)phenyl)(piperidin-1-yl)methanone;
3-((5-chloro-2-hydroxyphenyl)(4-(4-methoxyphenyl)piperazin-1-yl)methyl)-N-cyclopentylbenzamide;
2-((4-(benzyloxy)-3-fluorophenyl)(4-(4-methoxyphenyl)piperazin-1-yl)methyl)-4-chlorophenol;
2-((4-(benzyloxy)-3-fluorophenyl)(4-(6-fluorobenzo[d]isoxazol-3-yl)piperidin-1-yl)methyl)phenol;
2-((4-(2, 3-dichlorophenyl)piperazin-1-yl)(o-tolyl)methyl)phenol;
N-cyclopentyl-3-((4-(2,3-dichlorophenyl)piperazin-1-yl)(2 hydroxyphenyl)methyl)benzamide; and
2-((4-(benzyloxy)-3-fluorophenyl)(4-(2,3-dichlorophenyl)piperazin-1-yl)methyl)phenol.

Physical data for the title compound

Reagents		Product	Yield
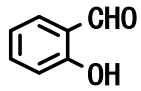 1a	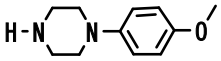 2a	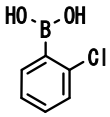 3a	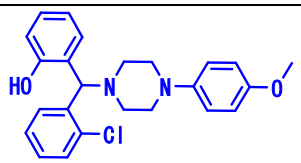 4a	85
1a	2a	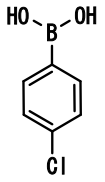 3b	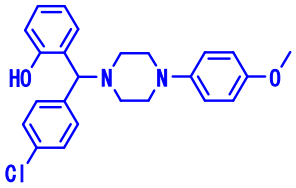 4b	85
1a	2a	 3c	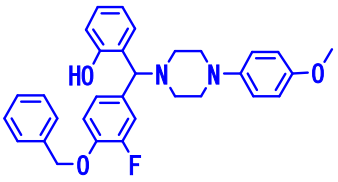 4c	95
1a	2a	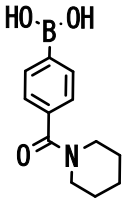 3d	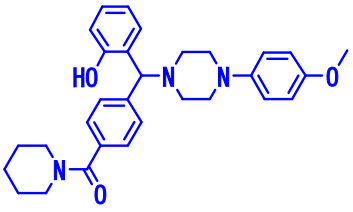 4d	90
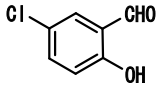 1b	2a	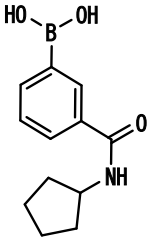 3e	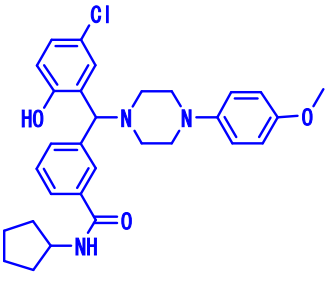 4e	85

1b	2a	3c	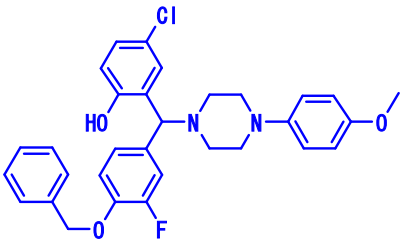 4f	90
1a	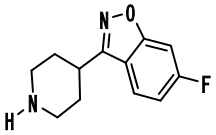 2b	3c	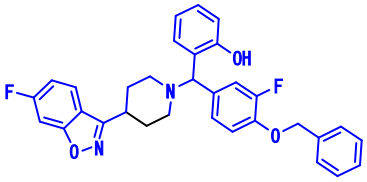 4g	90
1a	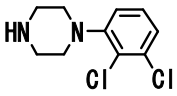 2c	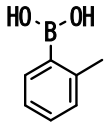 3f	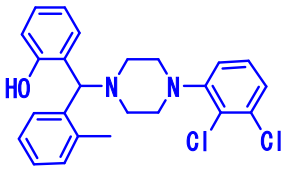 4h	80
1a	2c	3e	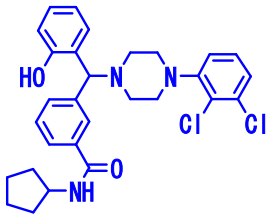 4i	90
1a	2c	3c	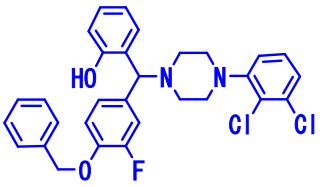 4j	90

Experimental Section:

General preparation of NC-Compounds:

Piperazines (0.8mmol) and salicylaldehyde (0.8mmol) was taken in an RBF and was stirred for 10 minutes using Dioxane as solvent. After 10 minutes,Aryl boronic acid (0.8mmol) was added to the mixture and was refluxed with continuous stirring for 8hrs using Dioxane as solvent on a hot plate maintained at 90^0C.After 8hrs, ethyl acetate and water was added to the

reaction mixture, ethyl acetate layer was separated using separating funnel and dried over anhydrous sodium sulfate .Ethyl acetate was evaporated to obtain the product. The desired phenolic compounds product was obtained by separation using column chromatography.

4a :(2-chlorophenyl)(4-(4-methoxyphenyl)piperazin-1-yl)methyl)phenol;^{1}H NMR(CDCl3, 400 MHz) δ: 3.691(s, 3H), 5.303(s, 1H,C-H), 1.184-3.691(m, 8H-piperazine protons), 7.597-7.615(d, 1H, J=7.2 Hz), 7.341-7.323(d,1H, J=7.2 Hz), 7.060-7.189(m, 4H-ArH), 6.555-6.815(m,5H-ArH), 6.956-6.974, (d,1H, J=7.2Hz)11.85(s, 1H-OH brd peak);^{13}C NMR (400 MHz, CDCl3)δ: 50.854, 55.521, 69.50, 114.45, 117.17, 118.44, 119.547, 122.05, 127.78, 128.83, 129.01, 129.19, 129.84, 129.93, 133.89, 145.11, 156.60; Melting point 120-124^{0}C.

4b :2-((4-chlorophenyl)(4-(4-methoxyphenyl)piperazin-1-yl)methyl)phenol;^{1}H NMR(CDCl3, 400 MHz) δ:2.539-3.065(m, 8H), 3.674(s, 3H), 4.359(s, 1H), 6.651(m, 1H), 6.740-6.804(m, 5H), 6.855-6.872(d, 1H, J=6.8Hz), 7.086(m, 1H), 7.165(m, 2H), 7.280(m, 1H), 7.361(m, 1H); ^{13}C NMR (400 MHz, CDCl3)δ: 50.74, 51.76, 55.52, 75.86, 114.49, 117.24, 118.43, 119.62, 124.41, 126.58, 128.28, 128.54, 128.92, 129.20, 130.28, 134.66, 141.63, 145.07, 154, 156.18; Melting point 85-89^{0}C.

4c :2-((4-(benzyloxy)-3-fluorophenyl)(4-(4-methoxyphenyl)piperazin-1-yl)methyl)phenol;^{1}H NMR(CDCl3, 400 MHz) δ: 1.194-3.079(m,8H), 3.689(s, 3H), 4.336(s, 1H), 5.041(s, 2H), 6.672-6.702(m, 1H), 6.781-6.819(m, 5H), 6.863-6.867(m, 2H), 7.026-7.082(m, 2H), 7.196(m, 1H), 7.279-7.348(m, 5H); ^{13}C NMR (400 MHz, CDCl3)δ: 50.770, 55.52, 71.26, 75.36, 114.46, 115.46, 117.16, 118.42, 119.54, 124.82, 127.34, 128.14, 128.62, 128.76, 129.14, 145.04, 156.14; Melting point 72-76^{0}C.

4d :(4-((2-hydroxyphenyl)(4-(4-Methoxyphenyl)piperazinyl)methyl)phenyl)(piperidin-1-yl)methanone;^{1}H NMR(CDCl3, 400 MHz) δ: 1.183-2.469(m, 10H), 2.557-3.684(m, 8H), 3.684(s, 3H), 4.412(s, 1H), 6.631(m, 2H), 6.745-6.813(m, 4H), 7.059-7.095(m, 1H), 7.191-7.216(m, 1H), 7.261-7.269(m, 2H), 7.351-7.409(m, 2H); ^{13}C NMR (400 MHz, CDCl3)δ: 24.51, 26.525, 29.68, 43.60, 48.73, 50.71, 51.80, 55.51, 76.04, 114.45, 117.134, 118.366, 119.198, 119.52, 124.75, 126.74, 127.50, 128.04, 128.50, 128.79, 129.29, 136.18, 141.02, 145, 154, 156.2, 169.79(C=O); Melting point 78-82^{0}C.

4e :3-((5-chloro-2-hydroxyphenyl)(4-(4-methoxyphenyl)piperazin-1-yl)methyl)-N-cyclopentylbenzamide;^{1}H NMR(CDCl3, 400 MHz) δ: 1.186-1.650(m, 8H), 1.978-3.633(m, 8H), 3.689(s, 3H), 4.298-4.345(m, 1H), 4.421(s, 1H), 5.979-5.992(s, 1H) 6.736-6.803(m, 5H), 6.860(m, 1H), 7.192(s, 1H), 7.737(s, 1H), 7.304-7.339(m, 1H), 7.540-7.557(m, 2H); ^{13}C NMR

(400 MHz, CDCl3)δ: 23.79, 33.18, 50.67, 51.83, 55.51, 67.06, 75.06, 114.46, 118.45, 118.58, 124.02, 126.11, 126.42, 128.72, 128.87, 129.39, 139.39, 144.89, 154.19, 154.95, 166.68; Melting point 102-106^{0}C.

4f :2-((4-(benzyloxy)-3-fluorophenyl)(4-(4-methoxyphenyl)piperazin-1-yl)methyl)-4-chlorophenol;^{1}H NMR(CDCl3, 400 MHz) δ:1.179-3.620(m, 8H), 3.676(s, 3H), 4.261(s, 1H), 5.029(s, 2H), 6.716-6.791(m, 5H), 6.823(m, 1H), 6.862-6.882(m, 1H), 6.973-7.015(m, 2H), 7.110-7.139(m, 1H), 7.243-7.258(m, 2H), 7.280-7.317(m, 1H), 7.331-7.350(m, 2H); ^{13}C NMR (400 MHz, CDCl3)δ: 50.70, 51.59, 55.52, 71.27, 74.93, 114.48, 115.52, 118.58, 123.97, 124.39, 126.3, 127.3, 128.2, 128.8, 132.1, 136.27, 144.96, 146.74, 154.19, 154.93; Melting point 60-64^{0}C.

4g :2-((4-(benzyloxy)-3-fluorophenyl)(4-(6-fluorobenzo[d]isoxazol-3-yl)piperidin-1-yl)methyl)phenol;^{1}H NMR(CDCl3, 400 MHz) δ: 2.648-3.820 (m, 8H) 4.245(s, 1H), 5.009(s, 1H), 5.651(s, 2H), 7.276(s, 1H), 7.436-7.485(m, 3H), 7.606-7.682(m, 3H), 7.797(m, 2H), 7.876-7.954(m, 5H), 8.185(s, 1H); ^{13}C NMR (400 MHz, CDCl3)δ: 30.972, 50.76, 67.60, 71.79, 75.85, 98.16, 100.9, 104.9, 113.16, 115.97, 117.65, 119.96, 122.84, 125.4, 127.8, 128.6, 129.1, 129.6, 133.2, 136.8, 157.06, 160.87, 164.51, 165.86; Melting point 58-62^{0}C.

4h :2-((4-(2, 3-dichlorophenyl)piperazin-1-yl)(o-tolyl)methyl)phenol;^{1}H NMR(CDCl3, 400 MHz) δ: 2.479(s, 3H), 4.927(s, 1H), 2.260-3.063(m, 8H), 6.533-6.551(d, 1H, J=7.2Hz), 6.631-6.692(m, 2H), 6.739-6.758(d, 1H, J=7.6Hz), 6.789-6.809(d, 1H ,J=8Hz), 6.864(m, 3H), 7.092-7.183(m, 1H), 7.281-7.297(m, 1H), 7.537-7.552(d, 1H, J=6Hz); ^{13}C NMR (400 MHz, CDCl3) δ: 20.92, 51.16, 51.42, 73.44, 116.07, 116.96, 117.14, 118.716, 119.27, 119.83, 124.965, 125.24, 126.445, 127.12, 127.545, 128.266, 128.729, 129.260, 130.869, 134.072, 138.171, 150.600, 156.443 Melting point 108-112^{0}C.

4i(NPB) :N-cyclopentyl-3-((4-(2,3-dichlorophenyl)piperazin-1-yl)(2-hydroxyphenyl)methyl)benzamide; ^{1}H NMR(CDCl3, 400 MHz) δ: 1.183-1.647(m, 8H), 2.019-3.067(m, 8H), 4.509(s, 1H), 4.312-4.327(m, 1H, NH), 5.965(s, 1H), 6.668(m, 1H), 6.801-6.896(m, 3H), 7.073-7.190(m, 3H), 7.305(m, 1H), 7.527-7.542(m, 2H), 7.770(s, 1H); ^{13}C NMR (400MHz, CDCl3)δ: 23.78, 33.18, 51.22, 51.78, 76.10, 117.14, 118.59, 119.67, 124.69, 124.98, 126.22, 127.53, 128.85, 129.29, 131.08, 134.08, 135.53, 140.28, 150.5, 156.1, 166.73;m/z (M+2 ,526.2,527.2) Melting point 174-178^{0}C.

4j :2-((4-(benzyloxy)-3-fluorophenyl)(4-(2,3-dichlorophenyl)piperazin-1-yl)methyl)phenol; ^{1}H NMR(CDCl3, 400 MHz) δ: 1.183-3.074(m, 8H), 4.361(s, 1H), 5.034(s, 2H), 6.658-6.694(t, 1H, J=7,2Hz), 6.768(m, 1H), 6.856-6.873(m, 3H), 7.023(m, 1H), 7.055-7.094(m, 3H), 7.164(m, 1H), 7.231(m, 1H), 7.266(m, 1H), 7.304(m, 1H), 7.322-7.355(m, 2H); ^{13}C NMR (400 MHz, CDCl3)δ: 51.264, 71.260, 75.434, 117.15, 118.6, 119.6, 124.8, 124.9, 127.3, 127.5, 128.1, 128.6, 128.8, 129.18, 150.5, 156.09; Melting point 75-80^{0}C.

Scanned Spectral Details

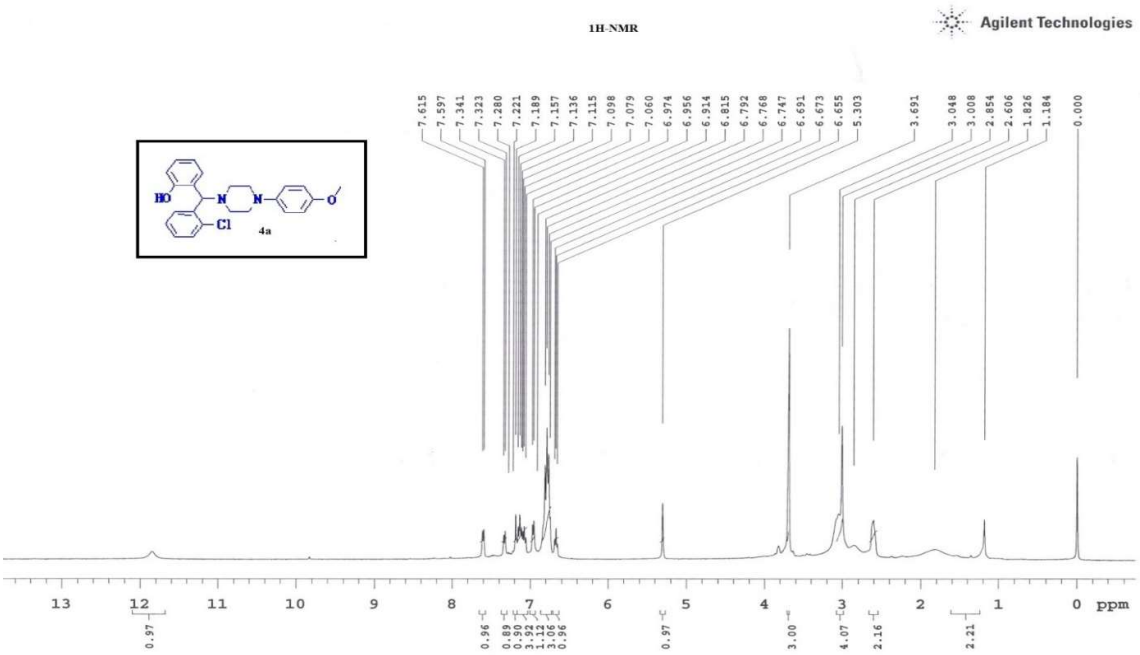

C-13 NMR

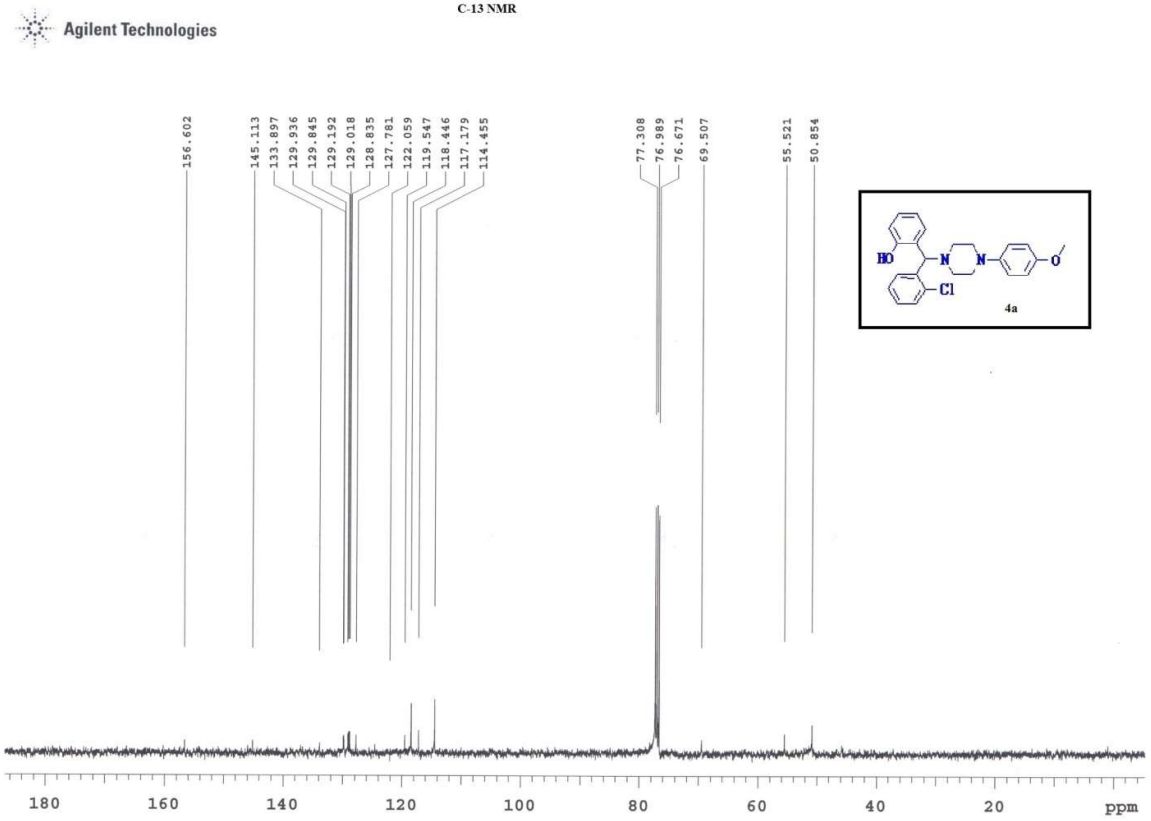

C-13 NMR

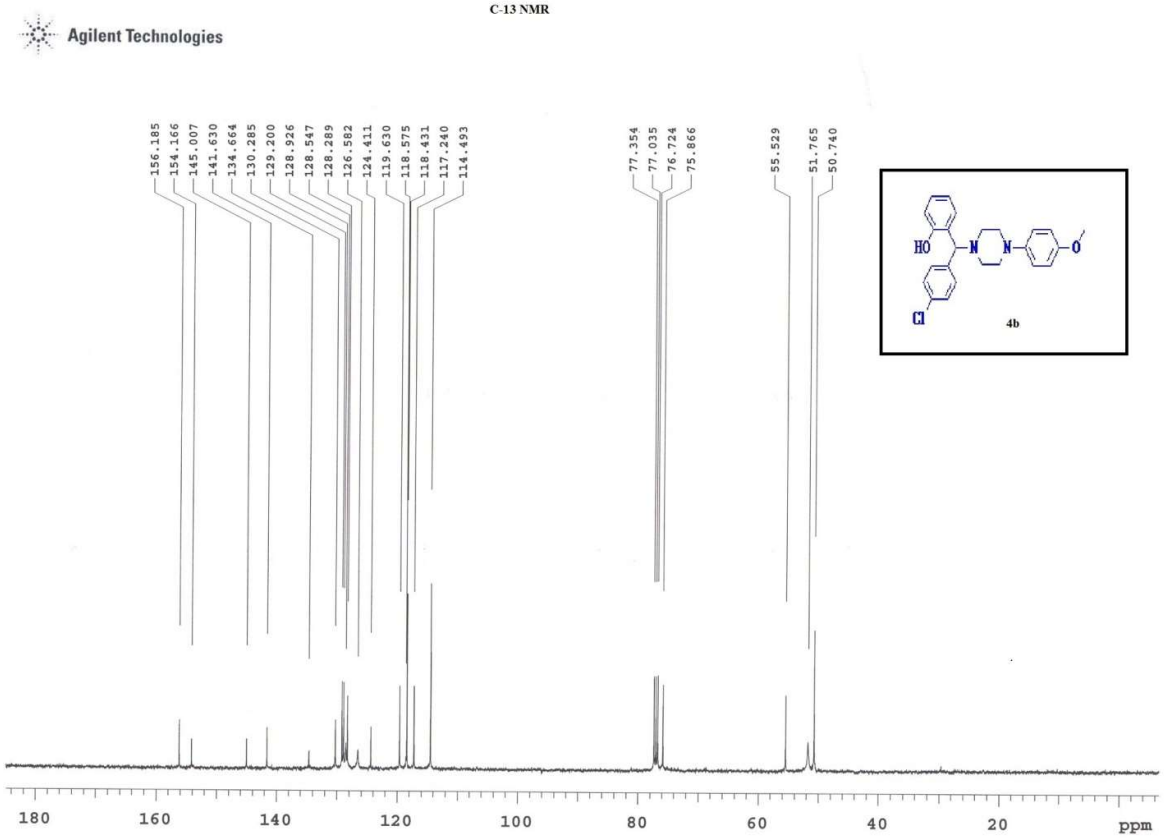

1H-NMR

Agilent Technologies

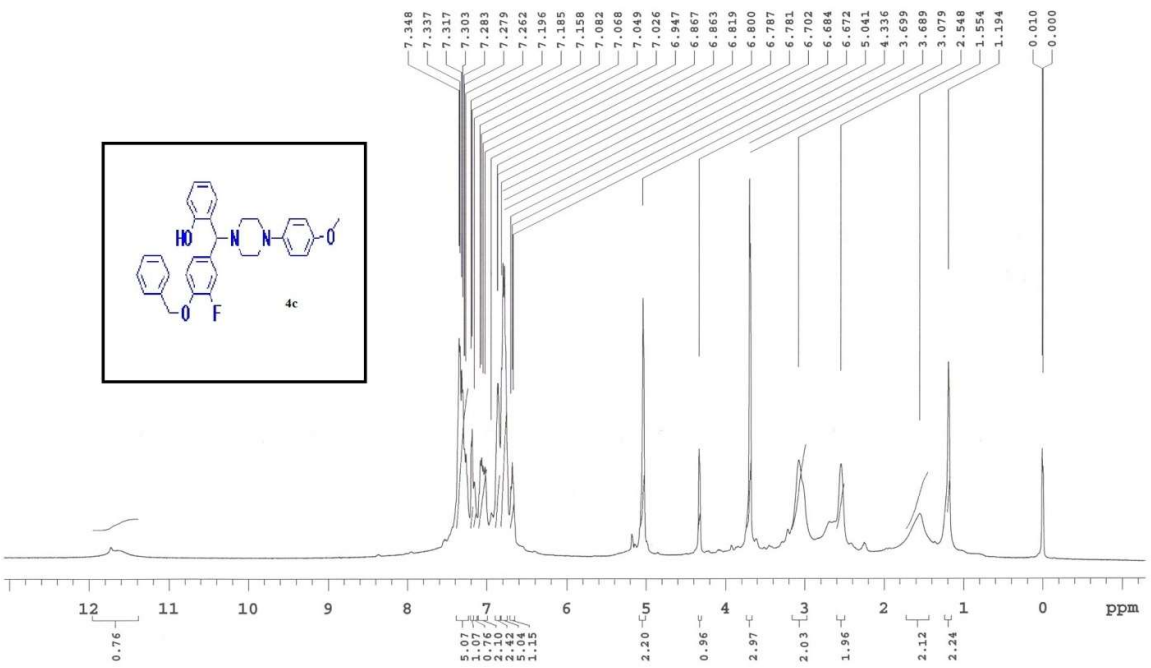

1H-NMR

Agilent Technologies

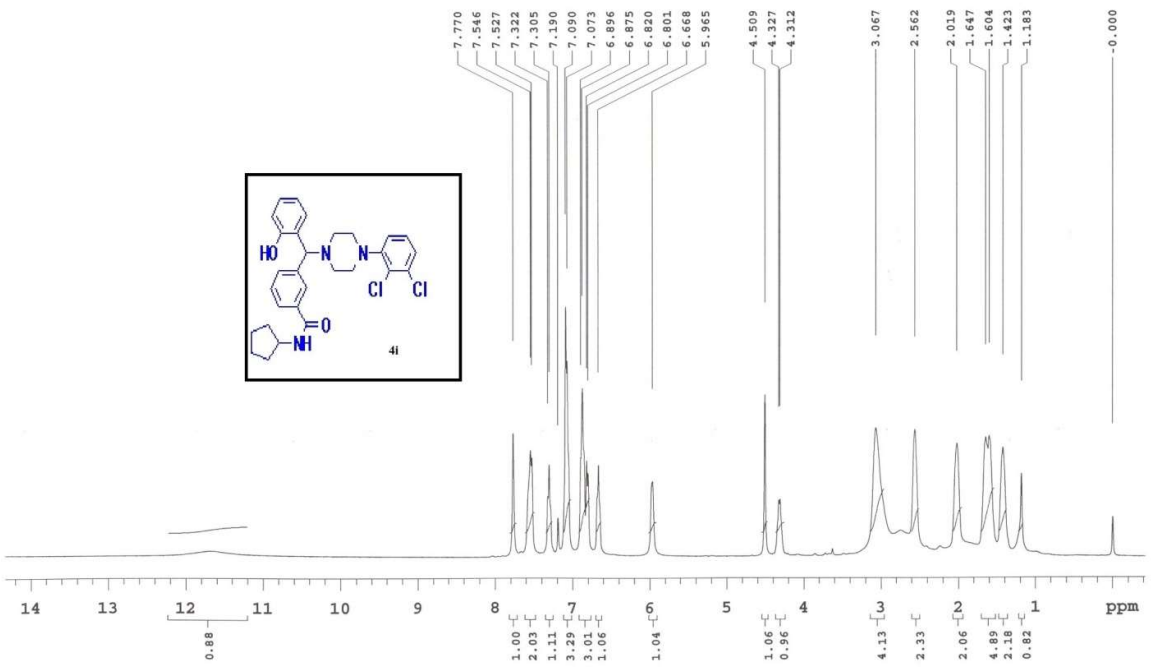

LCMS of 4i compound

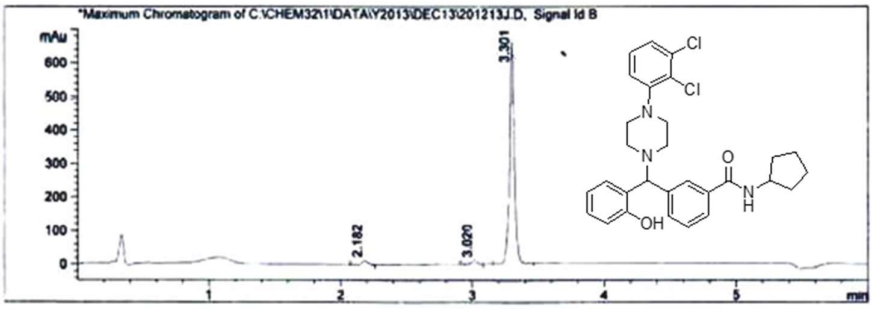

Peak No	RT min	Area	Area %
1	2.182	89.360	4.949
2	3.020	53.559	2.966
3	3.301	1662.763	92.085

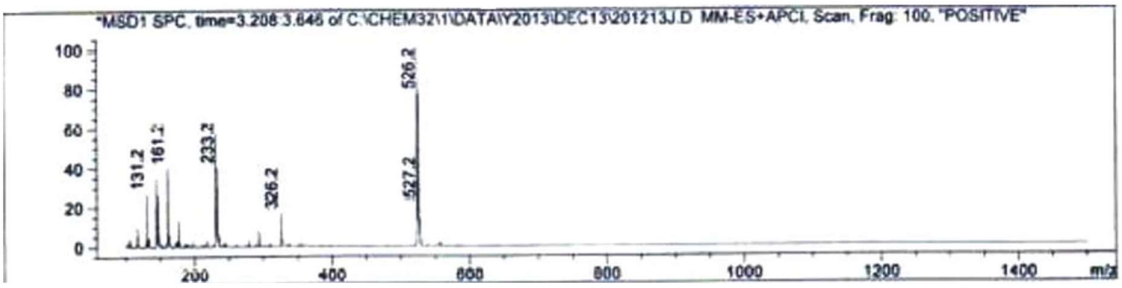

C-13 NMR

Agilent Technologies

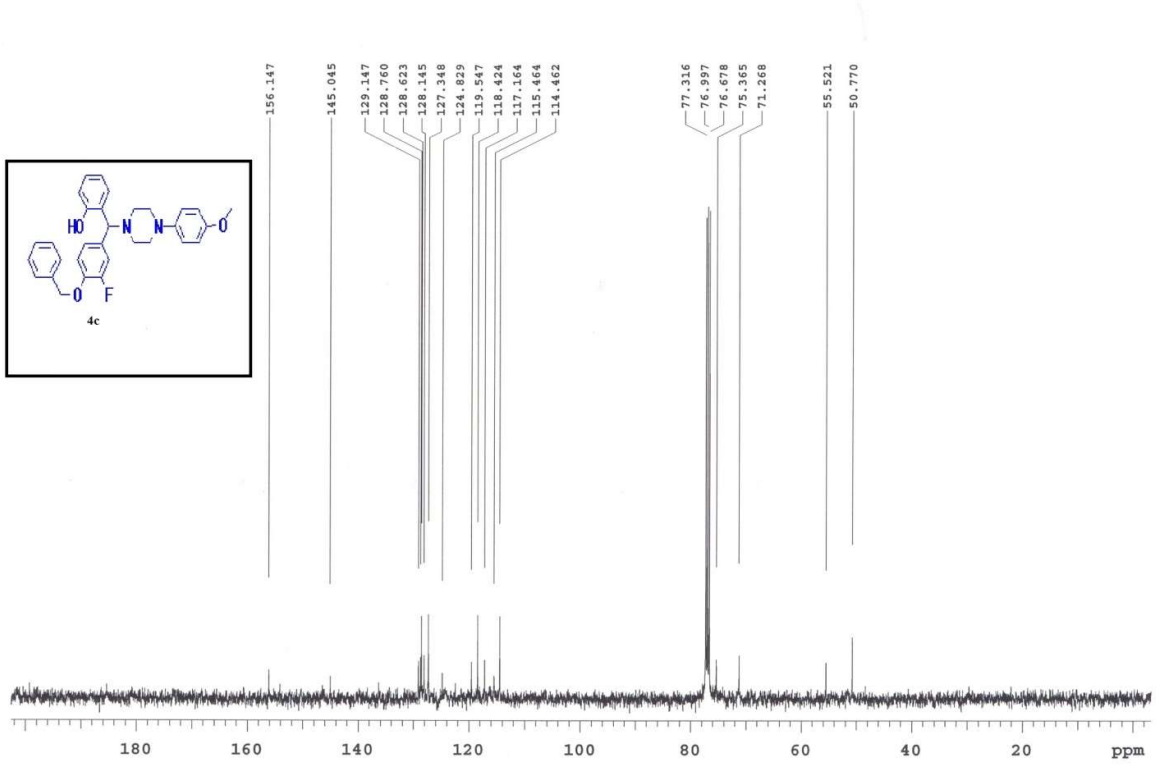

1H-NMR

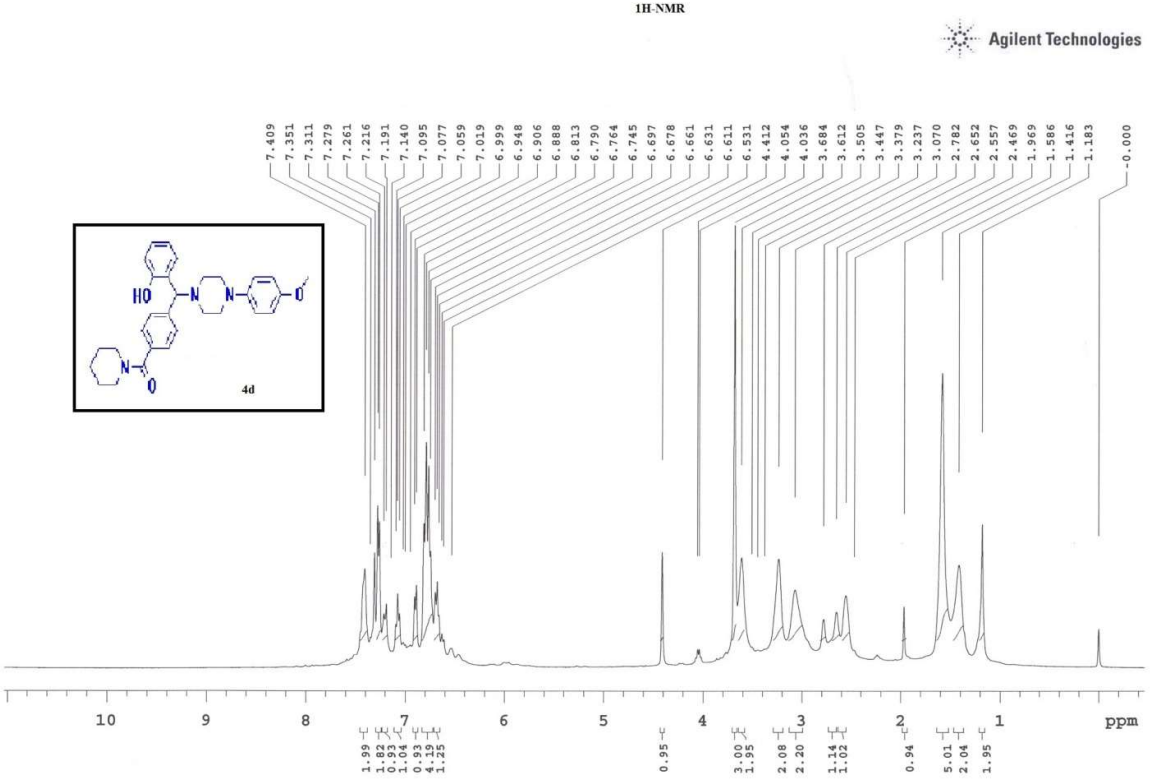

C-13 NMR

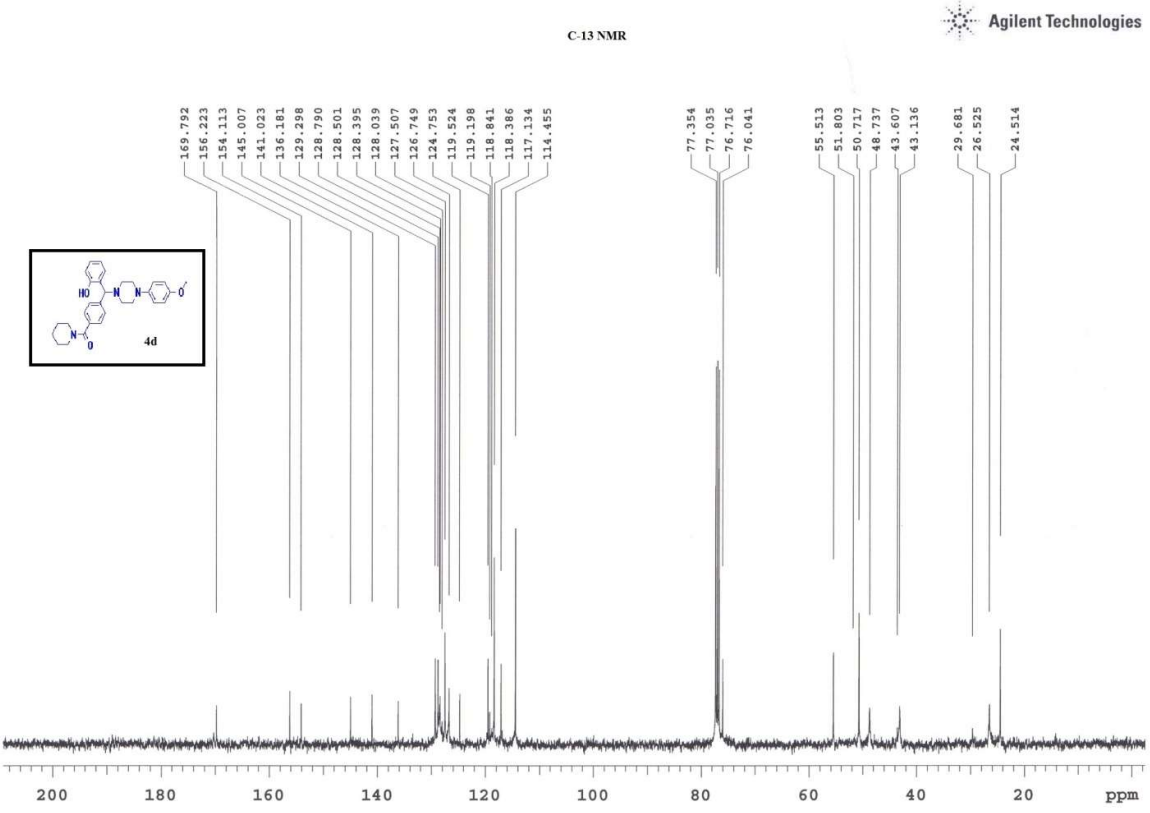

Agilent Technologies

C-13 NMR

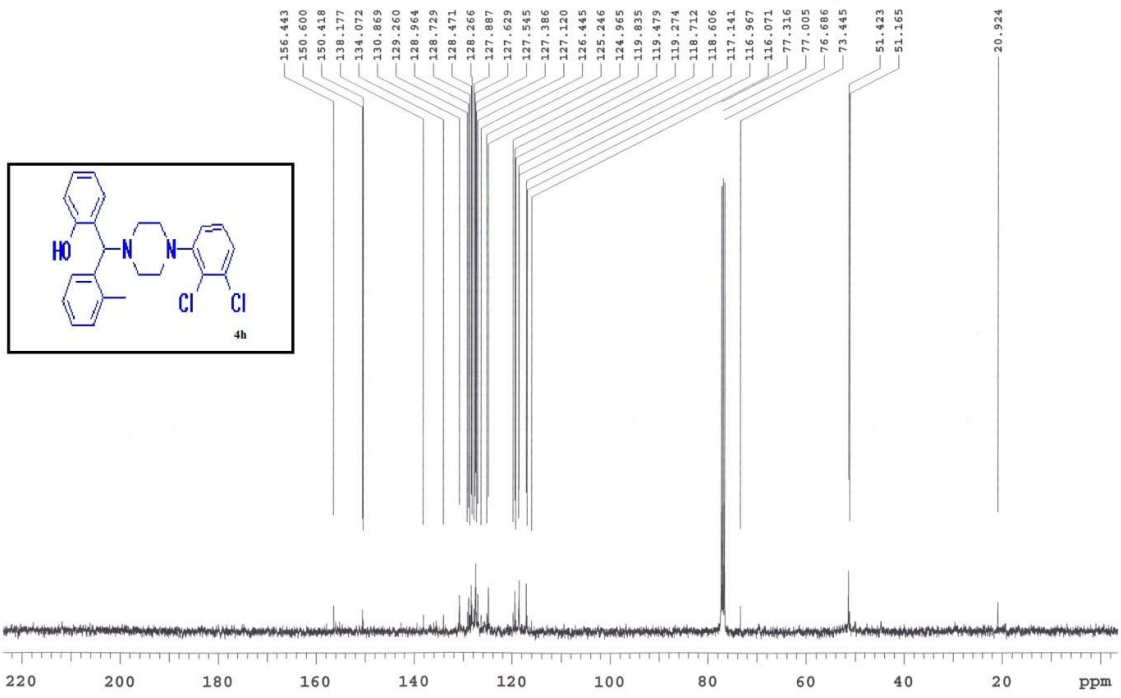

1H-NMR

Agilent Technologies

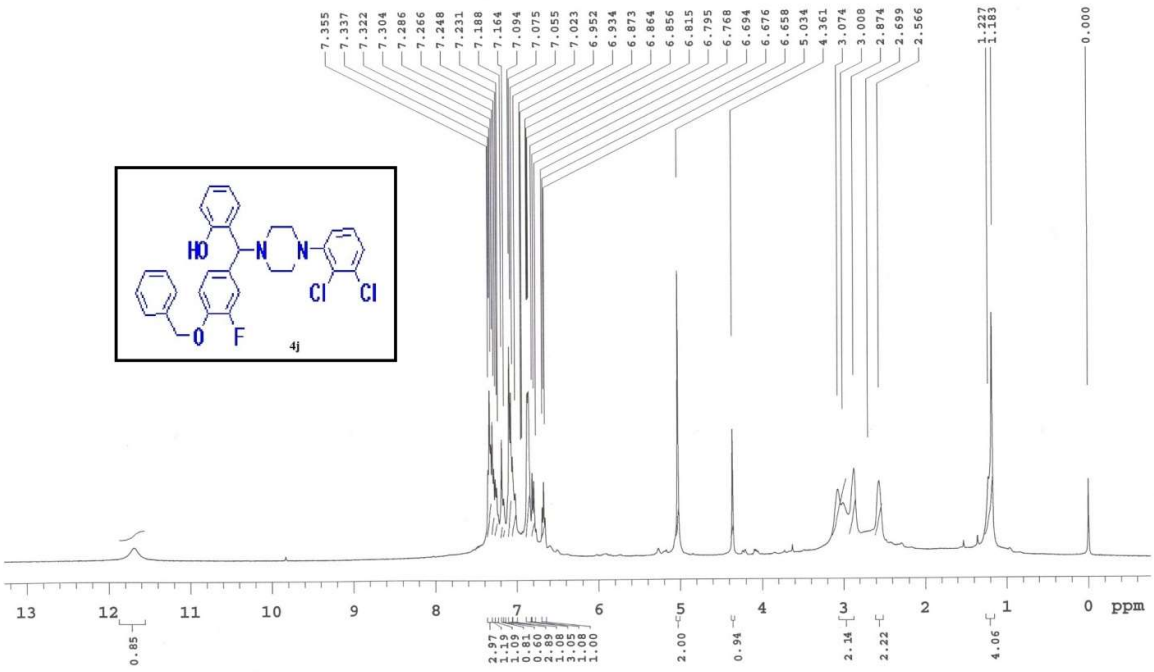

1H-NMR

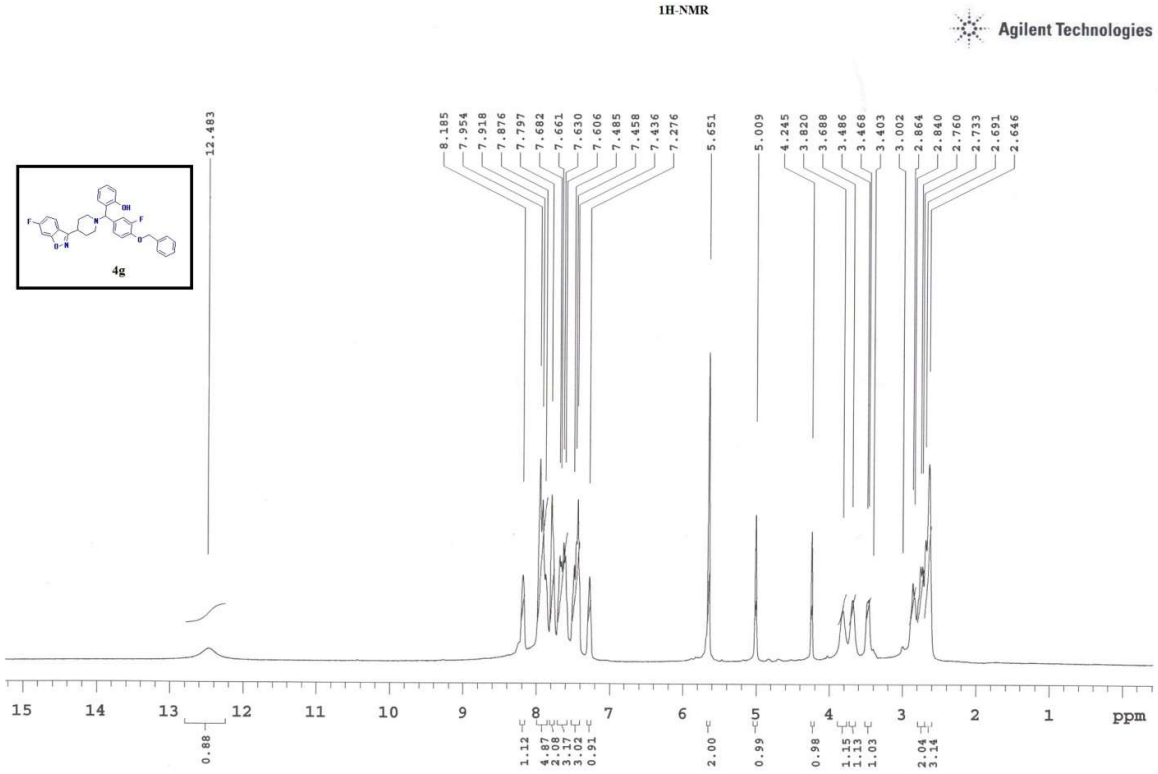

C-13 NMR

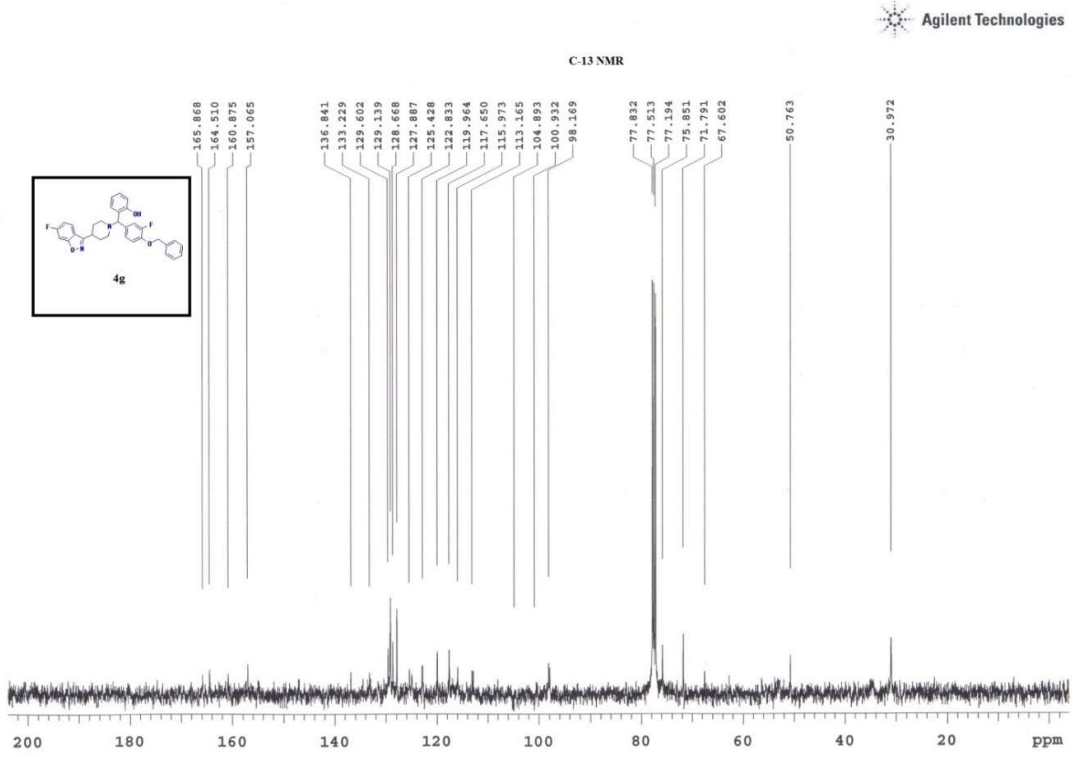

1H-NMR

Agilent Technologies

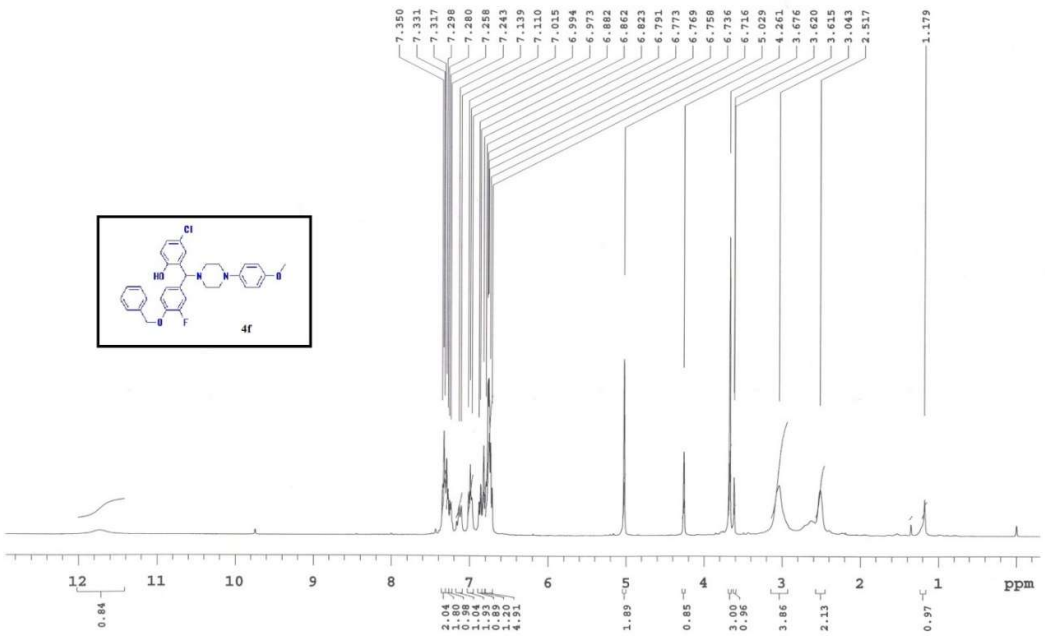

1H-NMR

Agilent Technologies

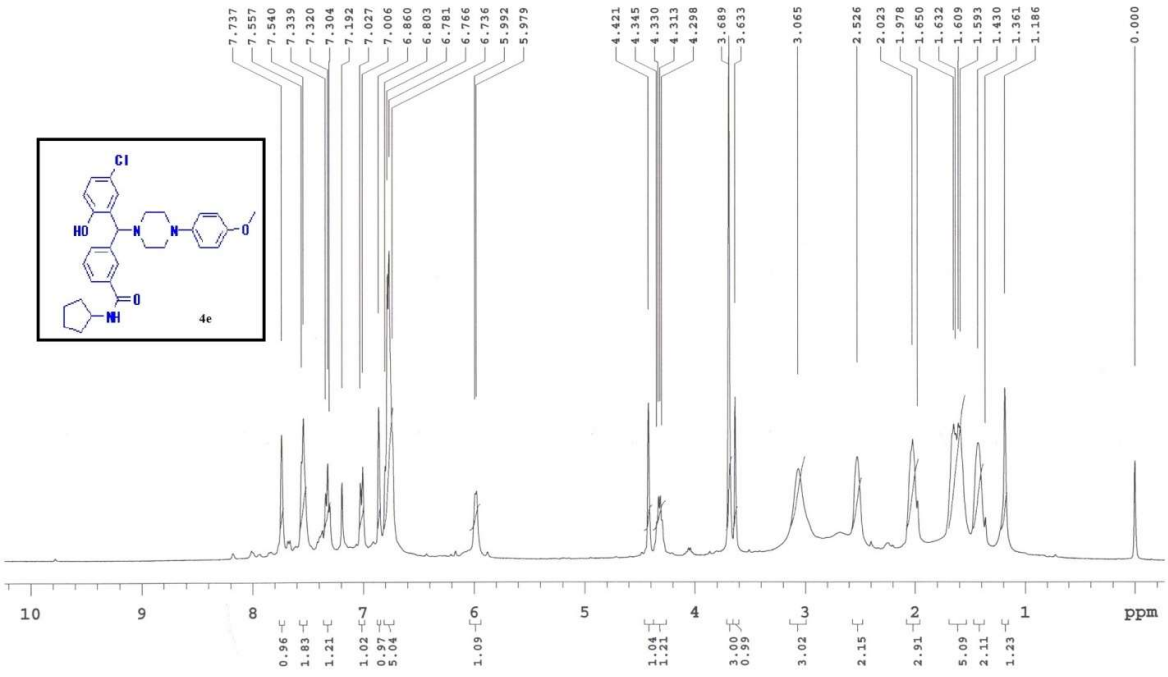

Agilent Technologies

C-13 NMR

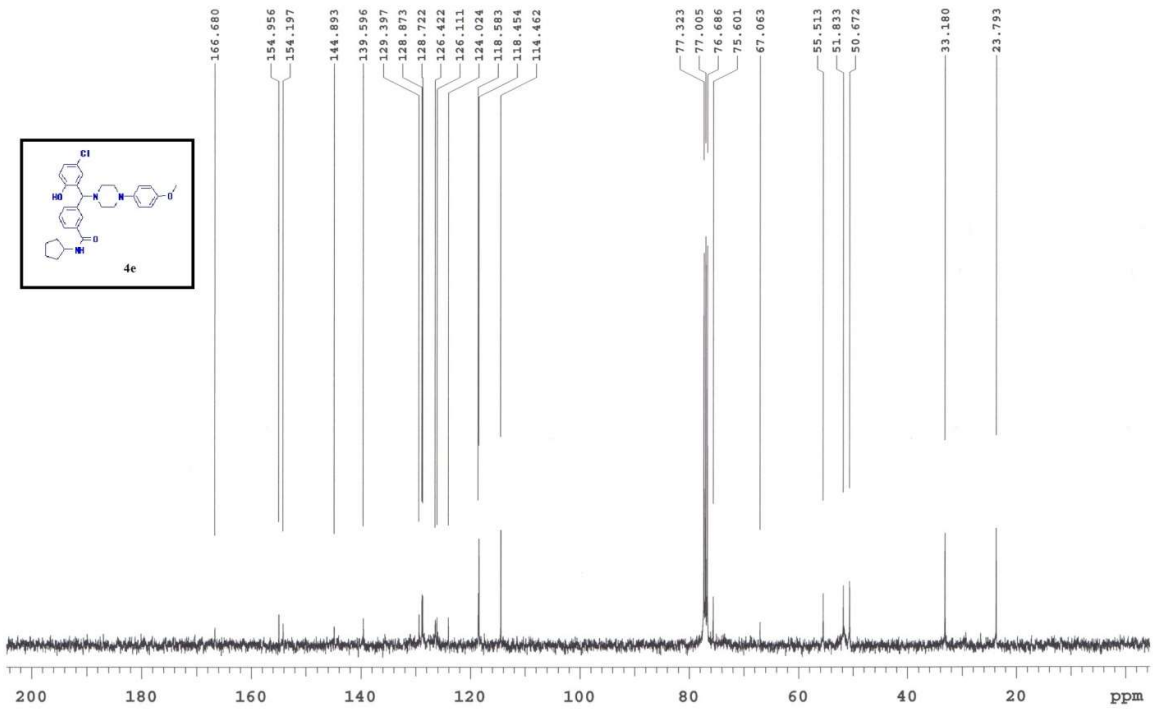

Supporting information 2:

(**A**) Cytotoxicity was evaluated using the ApoTox-Glo™ Triplex Assay Kit from Promega (www.promega.com/tbs/). Briefly, the ApoTox-Glo™ Triplex Assay combines three Promega assay chemistries to assess viability, cytotoxicity, and caspase activation events within a single assay well. The first part of the assay simultaneously measures two protease activities; one is a marker of cell viability, and the other is a marker of cytotoxicity. The live-cell protease activity is restricted to intact viable cells and is measured using a fluorogenic, cell-permeant, peptide substrate (glycylphenylalanyl-

aminofluorocoumarin; GF-AFC). The substrate enters intact cells where it is cleaved by the live-cell protease activity to generate a fluorescent signal proportional to the number of living cells. This live-cell protease becomes inactive upon loss of cell membrane integrity and leakage into the surrounding culture medium. A second, fluorogenic cell-impermeant peptide substrate (bis-alanylalanyl-phenylalanyl-rhodamine 110; bis-AAF-R110) is used to measure dead-cell protease activity, which is released from cells that have lost membrane integrity. Because bis-AAF-R110 is not cell-permeant, essentially no signal from this substrate is generated by intact, viable cells. The live- and dead-cell proteases produce different products, AFC and R110, which have different excitation and emission spectra, allowing them to be detected simultaneously. Statistical significance was assessed by an unpaired two-tailed *Student's t-test* using GraphPad Prism5. The column represents mean of triplicate determinations; bars, ±*SD*. $^{**}P < 0.001$, $^{*}P < 0.05$. **Note**: RFU, relative fluorescence unit; #; non-transformed, *immortalized* epithelial cells; MB-231, MDA-MB-231.

(**B**) Cell cycle analysis of MCF7 cells measured after treatment with 10μM NPB using flow cytometry analysis.

Supporting information 2:

A. Cytotoxicity

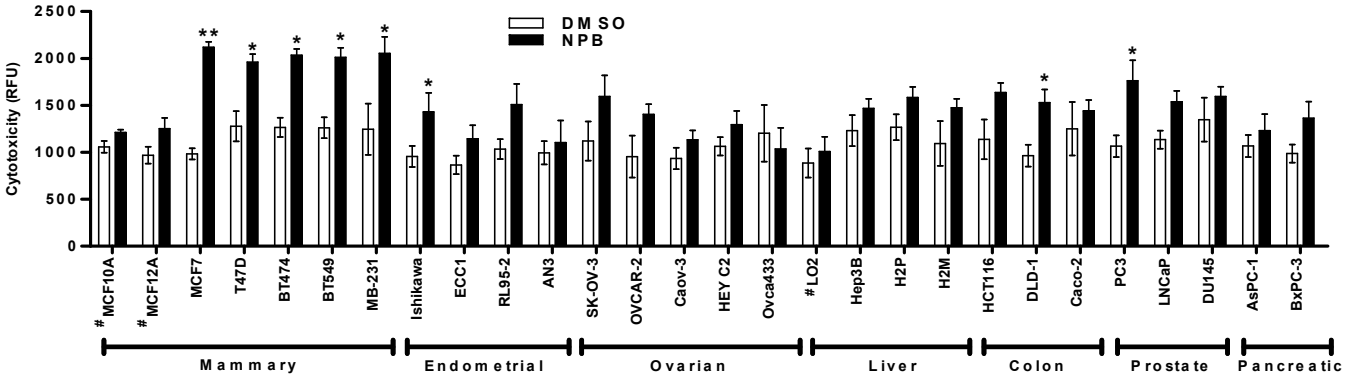

B. Cell cycle analysis

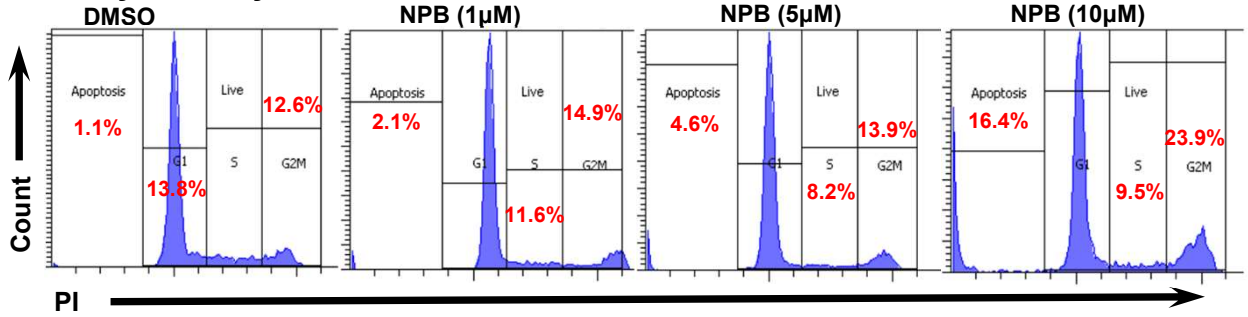

Supporting information 3: Predicted targets for the NPB compound.

Predicted targets for the compound NPB	Predicted probability for entry compound
D(3) dopamine receptor	24.3134661528
D(2) dopamine receptor	20.1296782952
Urotensin-2 receptor	14.6538320273
D(4) dopamine receptor	11.0013239465
Bcl2 antagonist of cell death	**5.58542701946**
5-hydroxytryptamine receptor 2A	5.46092273053
Alpha-2A adrenergic receptor	3.74857096194
Gastric inhibitory polypeptide receptor	3.11667843356
Kappa-type opioid receptor	2.21102306166
Apoptosis regulator Bcl-2	2.09283646379

Supporting information 4:

(**A**) Western blot analysis was used to assess the level of Ser99 phosphorylation of pBAD, BAD, pAKT, and AKT in MCF7 cells after an increasing period of treatment with NPB (10μM). Soluble whole cell extracts were run on an SDS-PAGE and immunoblotted as described in methodology. The sizes of detected protein bands in kDa are shown on the *left side*. (**B**) Kinases and phosphorylated substrates were detected using a Western Blot array (Proteome Profiler Human Phospho-Kinase Array Kit. MCF7 cells treated with NPB (10μM) or DMSO for 12h at 37^0C before preparation of cell lysate. Mean pixel density was analysed using ImageJ software and is represented *below*. (C) AKT kinase activity was detected using the Akt Kinase Activity Kit (Non-Radioactive) from Enzo Life Science, USA. MCF7 cells were treated with NPB (1, 5, and10μM) or DMSO (V) for 12h at 37^0C before preparation of cell lysate (*left side*). AKT inhibitor V (5μM) was used as control (C). Purified recombinant active Protein Kinas B (AKT) incubated with NPB (1, 5, and 10μM) or DMSO (D); or AKT inhibitor V (5μM) (as control, C) for 4h at 37^0C prior to initiating the kinase reaction (*right side*). Statistical significance was assessed using an unpaired two-tailed *Student's t-test* using GraphPad Prism5. The column represents mean of triplicate determinations; bars, ±*SD*. $**P < 0.001$, $*P < 0.05$.

Supporting information 4:

A. Western blot

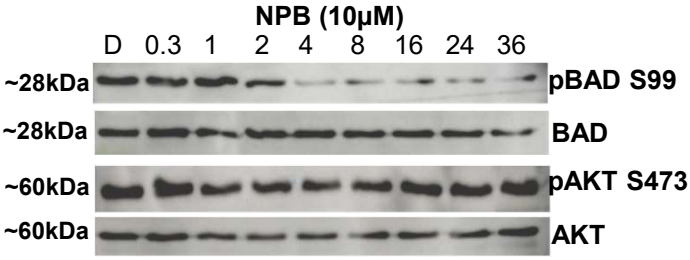

B. Kinase array

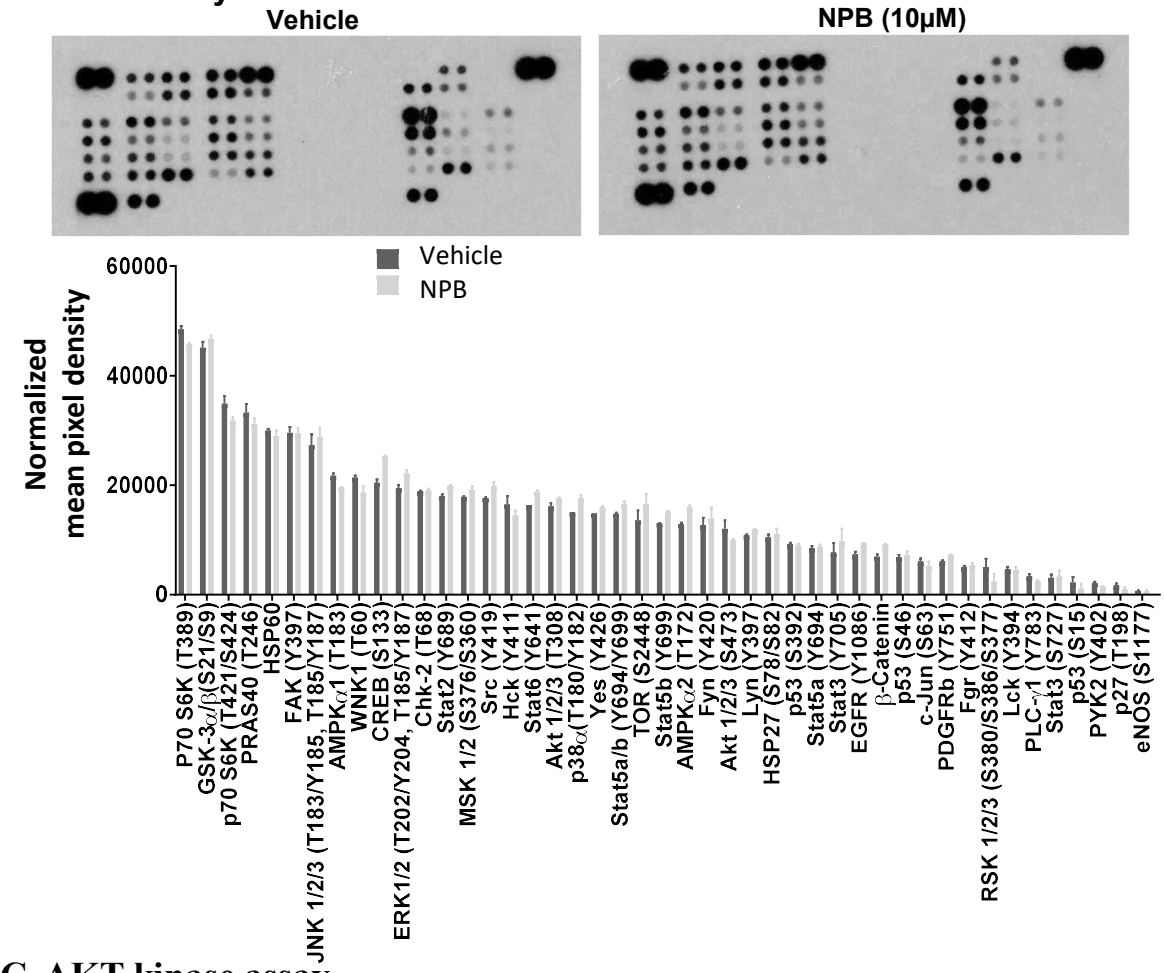

C. AKT kinase assay

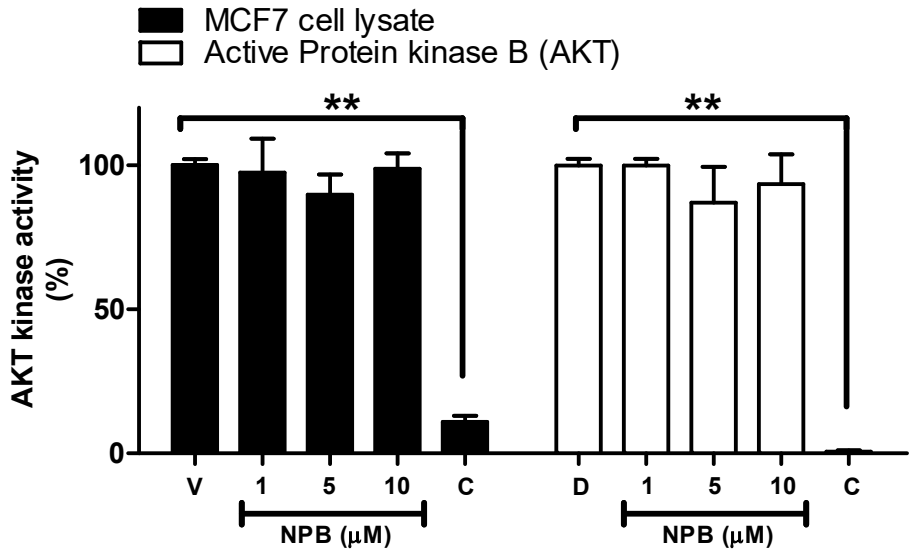

Supporting information 5: Pharmacokinetics of NPB.

(A) Plasma concentration of NPB after intravenous (IV, PK) (red) or oral (POPK) (blue) administration in Wistar rats. 2 mg/kg for IV or 10 mg/kg for oral of NPB suspension was prepared and administrated to rats. At appropriate time intervals, blood was collected, and the concentration of NPB in plasma was determined using HPLC. Results represent the mean ± *SD* of three animals. **(B)** Pharmacokinetic parameters of NPB in plasma after IV injection of 2 mg/kg in Wistar rats. **(C)** Pharmacokinetic parameters of NPB in plasma after oral administration of 10 mg/kg NPB to Wistar rats. AUC: Area Under the Plasma Concentration-Time Curve; AUC_{INF}: Area Under the Plasma Concentration-Time Curve from t=0 to infinity; $AUC_{\%Extrap}$ Percent Extrapolated AUC from t_{last} to infinity; C_{max} Peak concentration in plasma; CL: Plasma systemic Clearance; CL/F: Oral Clearance; F: Absolute Oral Bioavailability; T_{max}: Time of peak concentration in plasma; $t_{1/2}$: Elimination half-life; V_{ss}: Volume of Distribution at Steady-state; V/F Apparent volume of distribution estimated from Oral PK

Supplementary information 5

A. Pharmacokinetic profile of NPB

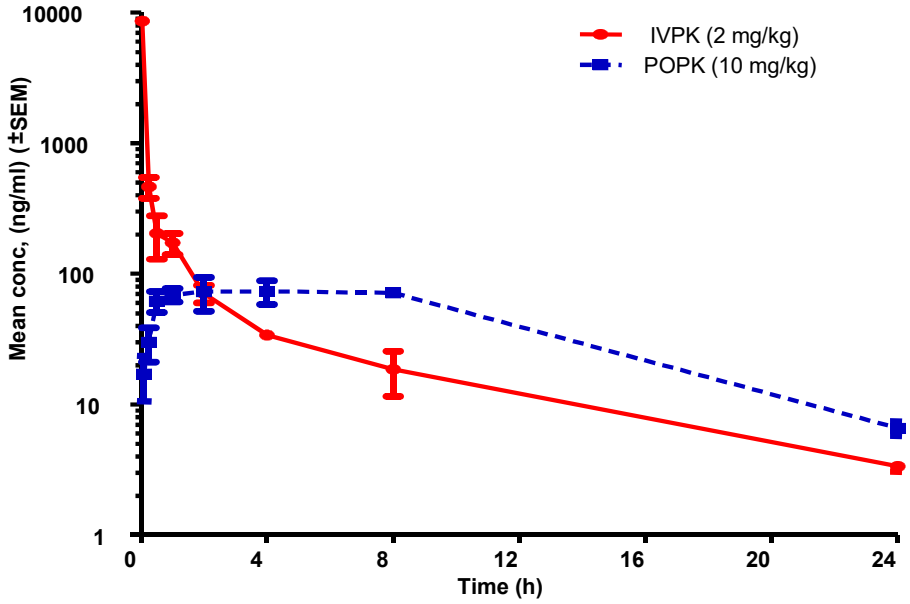

B. PK parameters of NPB in rats [IV, 2 mg/kg]

Parameter	Estimate
K_e (1/h)	0.11
$t_{1/2}$ (h)	6.13
AUC_{last} (h*ng/ml)	1598
AUC_{INF} (h*ng/ml)	1627
AUC[%Extrap]	1.80
CL (l/h/kg)	1.2
V_{ss} (l/kg)	3.1

C. PK parameters of NPB in rats [p.o., 10 mg/kg]

Parameter	Estimate
K_e (1/h)	0.13
$t_{1/2}$ (h)	5.39
T_{lag} (h)	0
T_{max} (h)	4
C_{max} (ng/ml)	73.4
AUC_{last} (h*ng/ml)	991
$AUC_{0-\infty}$ (h*ng/ml)	1045
$AUC_{\%Extrap}$ (%)	5.18
V_z/F (ml/kg)	74.4
CL/F(ml/h/kg)	9.6
F(%)	12.4*

Supporting information 6: Acute toxicity analysis

Eight weeks of age adult Swiss Albino/C57BL6J mice were used. Experimental animals were randomly divided into four groups with each group consisting of 5 mice. Group-I: Saline control, Group-II: Vehicle, Group-III: NPB (5mg/kg bodyweight) and Group-IV: NPB (20mg/kg body weight). Animals were IP. injected with saline/vehicle/NPB daily for eight days consecutively and monitored for the changes in body weight, toxicity, and potential mortality. On the 9^{th} day, animals were euthanized, and blood was collected *via* cardiac puncture, a portion of blood was mixed with anticoagulant immediately and remaining blood was allowed to clot and centrifuged at 1000*g* for 15 min to obtain serum. Kidneys, liver, spleen, and colon were harvested, rinsed with cold PBS and blotted free of blood, weighed and photographed.

For haematological studies, anti-coagulated blood was subjected to assess various haematological parameters (SI 6) using commercial kits as per manufacturer's instructions. Histological assessment was performed for liver, kidney, spleen, lung, stomach, colon and small intestinal tissues. The processed tissues were embedded in paraffin wax, and sections of 5µm thickness were prepared, stained with a hematoxylin-eosin dye (H&E) and observed under an Axio Imager A2 microscope (Oberkochen, Germany) and photographed.

(A) The left side represents the relative body weight in percentage from day 1 to day 8. The right side represents the percentage change in body weight on day 9. **(B)** Anti-coagulated blood was subjected to differential count to assess the possible effect of NPB on hematologic components. The figure presents differential count (WBC, RBC, PLT, Hb, and HCT) of mice treated with the two different dosages of NPB. **(C)** The acute toxicity effect of NPB on the liver was assessed by estimating the serum levels of ALT and AST. **(D)** The acute toxicity effect of NPB on kidney was assessed by estimating the level of BUN and activity of CK. **(E)** The acute

toxicity effect of NPB on tissue damage was assessed by estimating the level of activity of LDH.

Note: WBC, white blood cells; RBC, red blood cells; PLT, platelets; Hb, haemoglobin; HCT, haematocrit; ALT, alanine aminotransferase; AST, aspartate aminotransferase; BUN, blood urea nitrogen; CK, creatine kinase; and LDH, lactate dehydrogenase.

Supporting information 6:

A. Body weight

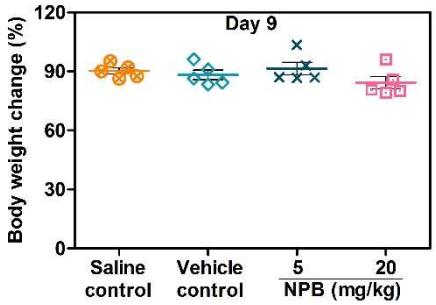

B. Hematology

	Saline control	Vehicle control	NPB (5 mg/kg)	NPB (20 mg/kg)
WBC (10^3/µL)	6.33 ± 0.09	5.33 ± 0.46	5.16 ± 0.61	5.76 ± 1.02
RBC (10^6/µL)	5.27 ± 0.22	5.75 ± 0.14	5.63 ± 0.17	5.65 ± 0.25
PLT (10^3/µL)	503 ± 63.29	463.33 ± 92.01	619.66 ± 50.23	553.33 ± 27.13
Hb (g/dL)	7.4 ± 0.44	7.63 ± 0.48	7.06 ± 0.68	7.13 ± 0.31
HCT (%)	29 ± 3.18	23.5 ± 1.61	22.9 ± 0.63	22.23 ± 0.59

Note: Results are presented as mean ± *SEM*; # *p value* = 0.0062 v/s vehicle control; *NC = not significant (*p*=0.390)

C. Hepatotoxicity

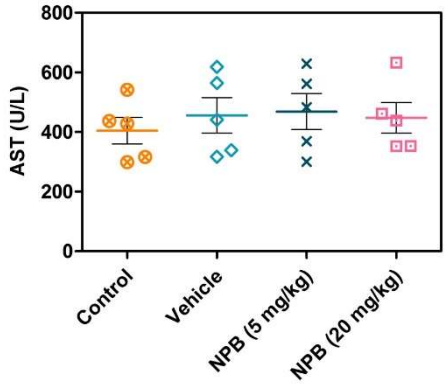

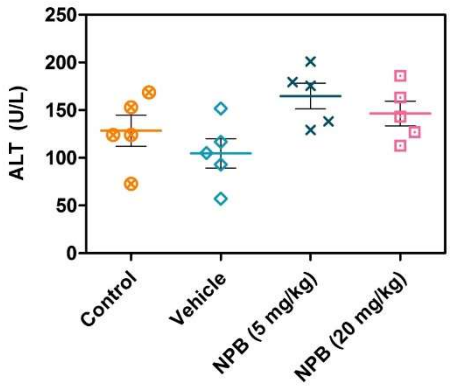

D. Renal toxicity

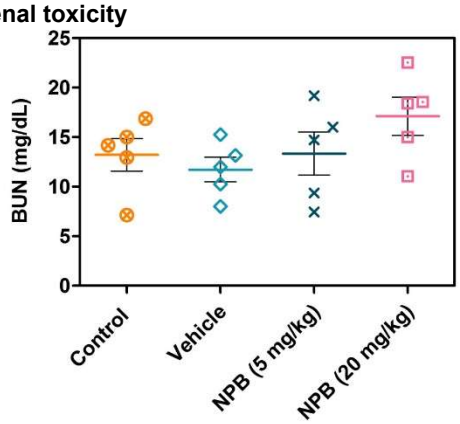

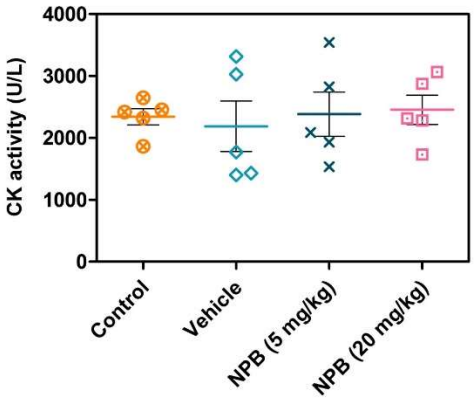

E. Cytotoxicity

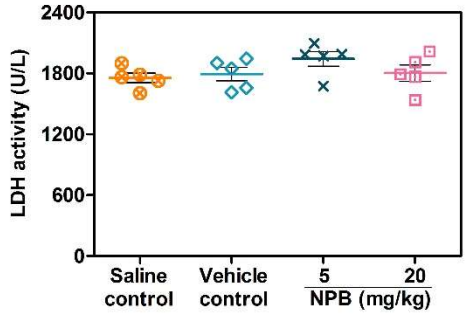

Supporting information 7: Acute cytotoxicity analysis.

(**A**) Liver weight of saline, vehicle, and NPB treated mice (*left)*. Macroscopic observation of liver and photomicrographs of H&E stained liver sections of saline, vehicle, and NPB treated mice (*right)*. (**B**) Spleen weight of saline, vehicle, and NPB treated mice (*left)*. Macroscopic observation of spleen and photomicrographs of H&E stained spleen sections of saline, vehicle, and NPB treated mice (*right).* (**C**) Kidney weight of saline, vehicle, and NPB treated mice (*left)*. Macroscopic observation of kidneys and photomicrographs of H&E stained kidney sections of saline, vehicle, and NPB treated mice (*right)*. **(D)** Photomicrographs of H&E stained lung sections of saline, vehicle, and NPB treated mice. **(E)** Photomicrographs of H&E stained stomach sections of saline, vehicle, and NPB treated mice.

Supporting information 7

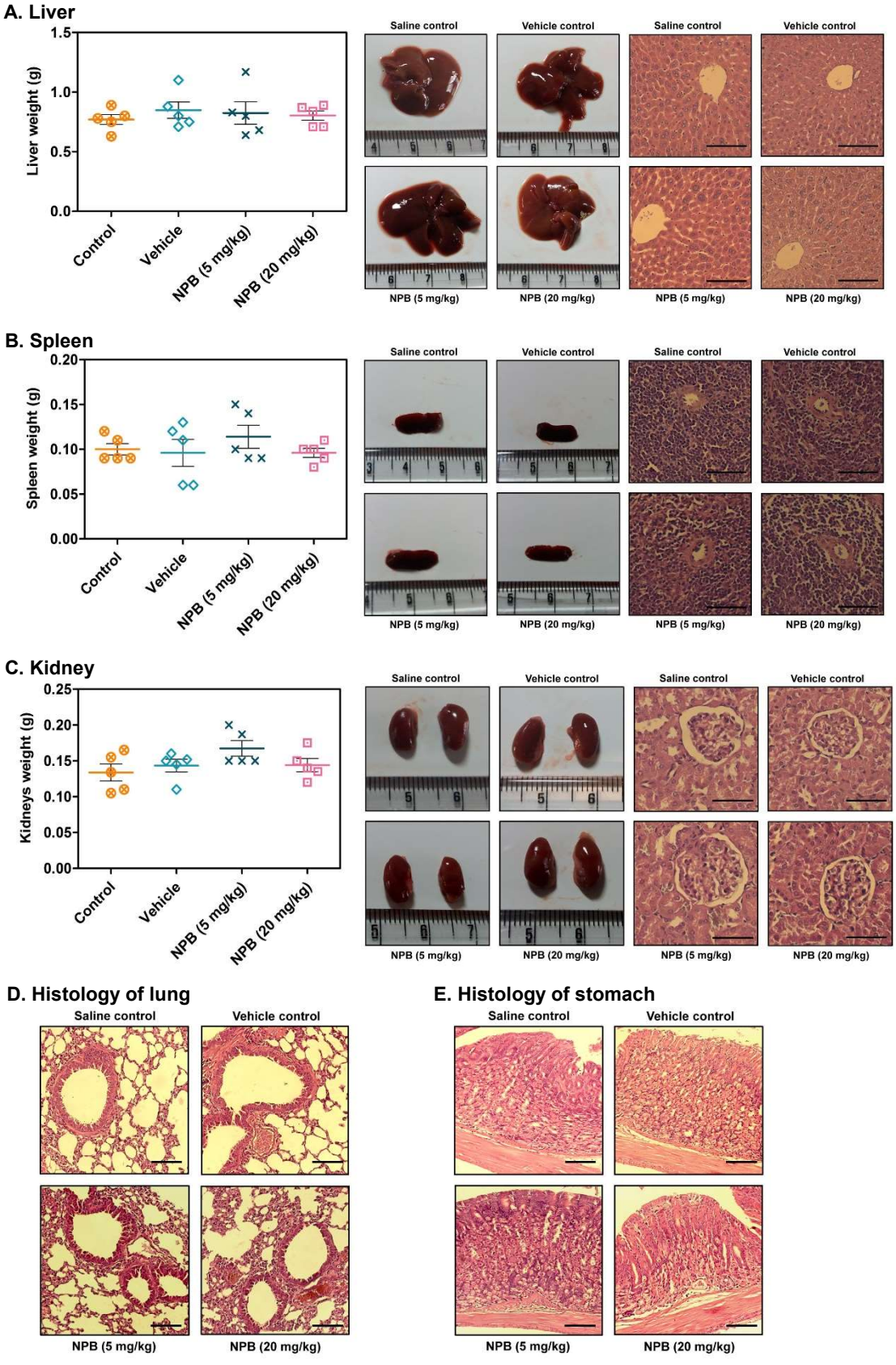

Supporting information 8: Acute cytotoxicity analysis

The effect of NPB on colon and small intestine after treatment with NPB.

(A) Colon length (above) and macroscopic observation of colon length (below) of saline, vehicle, and NPB treated mice. **(B)** Photomicrographs of H&E stained colon in saline, vehicle, and NPB treated mice. **(C)** Photomicrographs of the H&E stained small intestine in saline, vehicle, and NPB treated mice.

Supporting information 8:

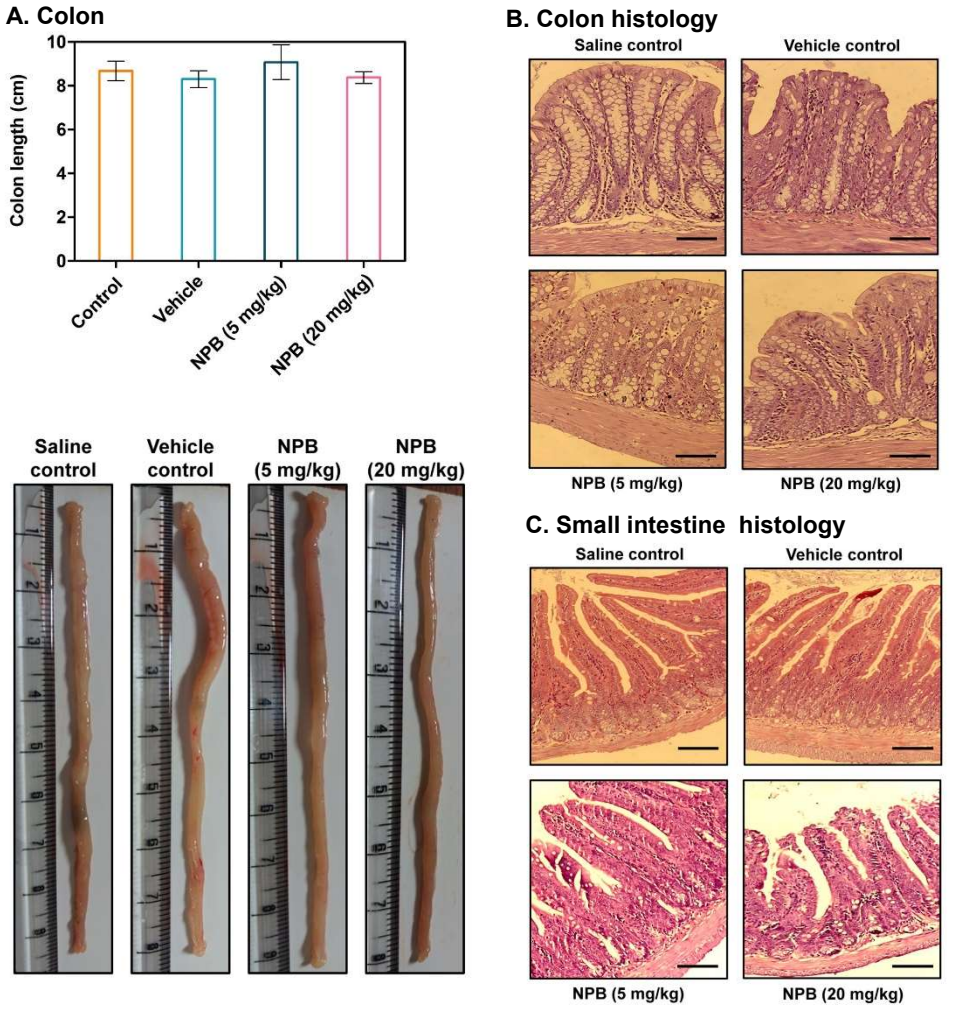

Supporting information 9

(A) Western blot analysis was used to assess the level of Bad Ser136 phosphorylation and total Bad protein in mouse mammary carcinoma cell lines (4T1 and 67NR) after treatment with increasing doses of NPB. Soluble whole cell extracts were run on an SDS-PAGE and immunoblotted as described in methodology. The sizes of detected protein bands in kDa are shown on the *left side.*

(**B**) Cell viability was evaluated using the AlamarBlue® viability assay. All assays were performed as described in methodology. IC_{50} values were calculated using GraphPad Prism5. The points represent mean of triplicate determinations; bars, ±*SD*.

Supporting information 9:

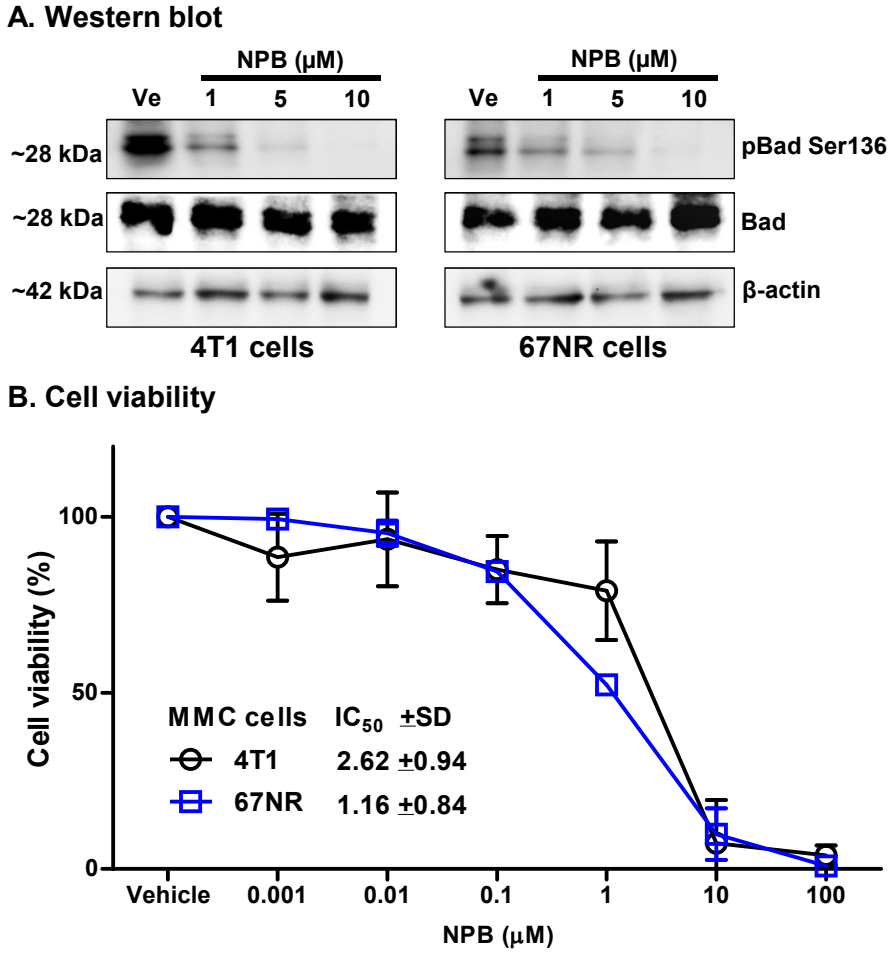

Supporting information 10:

Percentage (%) change in the density of BAD phosphorylation (Ser99), and BAD as determined from the western blot analysis of NPB treated xenograft tumours in Figure 7C. Density of blots were analyzed using ImageJ software from the NIH, USA *(*http://imagej.nih.gov/ij/*)*. The data are expressed as relative percentages normalized to β-ACTIN (mean ±SEM): *$p<0.05$ vs. vehicle.

Supporting information 10:

Percentage (%) change in the density of BAD phosphorylation (Ser99), and BAD as determined from the western blot analysis of NPB treated xenograft tumours in Figure 7C.